EPSC Abstracts
Vol. 5, EPSC2010-167, 2010
European Planetary Science Congress 2010

The study of Venus with amateur telescopes

D. Gasparri
Astronomy department, University of Bologna, via Ranzani 1 40127 Bologna, Italy (danielegasparri@yahoo.it)

Abstract

Near ultraviolet and infrared continuative high resolution images of Venus with amateur equipment can contribute actively to understand the dynamics of atmosphere and surface. In this paper images taken with a commercial 0.23 m Schmidt-Cassegrain telescope and CCD devices during 2007-2009 and 2010 elongations are discussed. Near ultraviolet and infrared sub-arcsecond resolution images of the clouds layers on the dayside have been analyzed, measuring the wind flow and showing change over time. The thermal emission of the nightside has been investigated at 965 nm and a topographic map of Phoebe and Beta regio built, with spatial resolution of 2.6" and temperature resolution of 5 K, then compared with Magellan radar altimetric data. Contrast and brightness variation caused by low clouds differential adsorbtion over the days have been observed.

1. Introduction

Venus and its atmosphere reveal properties and dynamics when observed in near UV [21] and IR light [2] . Because the position in the sky, with maximum elongations not greater than 48°, ground-based high resolution observations of Venus clouds from professional telescope have been difficult and not sufficient to answer to some questions regarding the dynamics of gaseous envelope. The super-rotation of upper atmosphere at near UV wavelengths was discovered only in 1954 by the amateur astronomer Charles Boyer [3][4]. Pioneer, Galileo, Messenger and Magellan spacecrafts provided a large amount of data, with excellent results [2][8][12][21]. A more continuative and high quality work is carried by the Venus Express mission, producing data on atmosphere and surface. [19] [18] In order to better understand the behaviour of atmospherical envelope and the evolution of the surface, and be a valid support to the Venus Express mission, a complete and long time lasting coverage of both clouds and surface from ground-based telescopes is advisable. With the development of digital devices accessible to the amateur community, good quality observations of Venus can be carried succesfully with a network of small size telescopes (typically 0.20 m) [13]. Amateur telescopes do not have time limitation and can observe also during daylight, producing results comparable, or better, to the larger professional telescopes, limited by seeing and geometrical conditions [7]. Sub-arcseconds images of upper atmosphere are achievable with at least a 0.20 m telescope (Fig.1), while the nightside thermal emission coming from the surface can be investigated at resolution of $\sim$ 2.5", revealing small temperature differences regulated by altitude [5] [16]. During 2007 and 2010 eastern elongations, the author imaged the planet dayside with a commercial 0.23 m telescope at near UV (380 nm) and near IR (965 nm) wavelength and the nightside thermal emission during 2009 elongation. Results are presented and the potential on an observative campaign done by the amateur community enforced [13].

2. Images acquisition

Dayside images were acquired by recording movies with exposures between 0.066 and 0.010 seconds, a common practice in planetary amateur astrophotography, with a sampling of 0.13"/px. Short exposures, and the subsequent selection of the best frames, mitigate the damage of atmospherical turbolence, giving often nearly diffraction limited images. During any observative session (duration of about 30 minutes), for any wavelength, 4 to 7 independent movies composed of $\sim$ 5000 frames were acquired, with different camera orientation. Best 2000 frames were selected from every movie, aligned and averaged. Resulting raw images were processed to enhance contrasts with unsharp masks and deconvolution filters. Final images of any session were compared in order to discover and avoid the presence of artefacts, which position, shape and magnitude change from one image to another. When the correspondence of the details gave a perfect matching, final IR and UV images of the session were built by averaging the processed images. Ultraviolet images were taken with a U Johnson photometric filter peacked at 365 nm and Violet W.47 filter with an IR-rejection, peacked at 380 nm. Although higher con-

trast with U filter, the greater light transmission of the W.47 let to use shorter exposures, giving better SNR images; the average resolution is 0.8" with some diffaction limited images (resolution better than 0.5") Fig.1.

Near infrared images were taken with a Schott RG1000 filter in the same observative sessions than UVs. The convolution of CCD spectral sensitivity with the filter band gave a gaussian curve peacked at 965 nm with FWHM of 120 nm and a peak QE of 0.03. Acquisition technique was the same. Infrared images have generally better quality, since the seeing improves with greater wavelengths and the background during daylight sessions is darker because the λ^{-4} trend of Rayleigh scattering from atmospherical gases.

Thermal radiation images were taken with a CCD camera ST-7XME set to a temperature of $T = 5.0 \pm 0.2$°C, exposures variable between 4 and 10 seconds and a sampling of 0.86 "/px. No occultation disk was used to hide the dayside. Observative sessions started 30 minutes after the sunset, until Venus reached an altitude of $\sim 10°$. The planet was oriented in acquisition stage with the line of dayside cusps parallel to the minor side of the CCD, in order to avoid the contamination of the nightside by dayside blooming. All frames were calibrated with master flat field and master dark frame. Data redundancy was guaranteed for each day by creating 2 indipendent raw images made of ~ 170 exposures. Contrast enhancment was performed with unsharp masks and Lucy-Richardson deconvolution, then the two processed images were averaged after details verification.

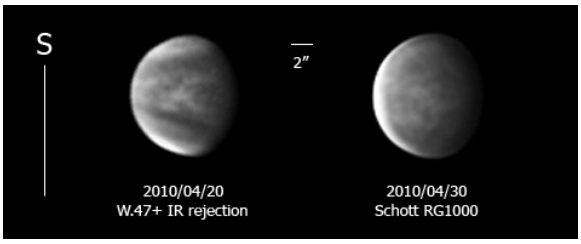

Figure 1: Diffraction limited images of Venus clouds at near UV (left) and near IR (right) light, taken during daylight sessions with the planet at 25° from the Sun, show the resolution limit of a 0.25 m telescope.

3. UV analysis

A total of 40 near UV images have been analyzed, 25 from 2007 eastern elongation (20 days) and 15 from 2010 eastern elongation (13 days). Winds speed was measured by analyzing cloud tracers in images separated by 180 to 240 minutes, and in two images by one equatorial rotation (93 hours), as follows. Every image was oriented with north celestial pole above, then a planetocentric fixed coordinates grid (not time dependent) was overimpressed. Longitudinal shift of tracers respect to the fixed grid was then measured. When the longitudinal shift $\Delta\lambda$ is known, in radiants, the linear velocity is given by:

$$v = \frac{Rcos(\phi)}{\Delta t}\Delta\lambda \qquad (1)$$

where R is the equatorial radius at clouds altitude [19], ϕ is the mean latitude of the selected feature and Δt the time interval between the images. Measurements were performed in 3 pair of images, along 5 latitude bands with amplitudes of $\Delta\phi \sim 4°$. Every measurement was repeated 3 times in order to lower the uncertainty on the position of the coordinate grid and the tracer. Data along the same latitudinal band were then averaged, reducing the uncertainties to ~ 20 m/s $(1-\sigma)$. According to preliminary velocities and equatorial period values, a better measurement, with a relative uncertainty of $dv/v \sim 0.05$, was performed on 2 images separated by 93 hours. Data are perfectly coerent with the previous; results are plotted in Fig. 2. Because the lacking of good quality tracers on images used, high latitudes were not mapped, but with constant and steady atmospherical conditions, measurements are possible until polar latitudes ($\phi \sim 70°$). The final rotational graph (Fig.2) shows a nearly constant trend in the range $-15° < \phi < 15°$, with an average value of $< v >= (110 \pm 5)$ m/s, in good agrement with Venus Express [19] and previous [12] data. The resulting rotational periods show a nearly solid body rotation of equatorial latitudes (Fig. 2), within the $1-\sigma$ uncerntainty of ~ 0.17 d. Mean equatorial period can be estimated by considering the average altitude of clouds ~ 66 km [19], with $1-\sigma$ error $1/N^{1/2}$ times the error on single measurement: $P = (3.91 \pm 0.05)$ d. This result agrees with Pioneer [21] and Venus Express [19].

According to mean rotational period, cylindrical maps of clouds coverage were built with images taken on consecutives days and phases greater than 0.6, showing changes during the time. Five complete projections have been assembled for the rotations 7-10, 16-19, 20-23, April 2007 and 6-9 and 25-28, April 2010. These data are sufficient to show some dynamical change of Venus upper atmosphere during time. Polar vortexes seem to have shape, size and

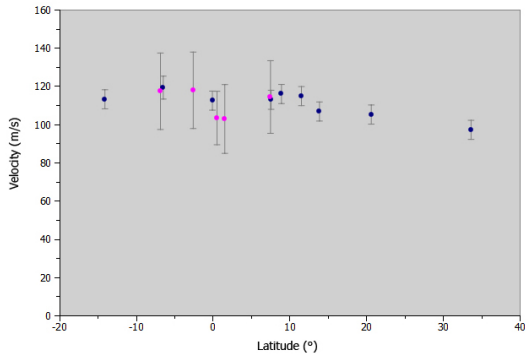

Figure 2: Winds speed at 380 nm. Red dots are the binning values of 3 pair of images at time interval of 180 and 240 minutes. Blue dots are the result of two images separated by 93 hours.

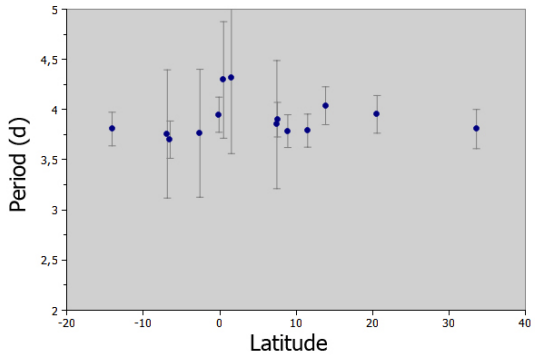

Figure 3: Plot of the rotational period as a fuction of latitude.

brightness variable with timescale of one-two weeks. Typical Y shaped equatorial cloud was visibile quasi-periodically at time interval of $\sim 8-12$ d. The cloud seems to originate from pole-ward motion of large dark clouds at $\phi = \pm 15°$ (Fig.4). The process evolves in less than 3 rotations. Small clouds, especially those bright, have life-time smaller than one rotation, while the larger and darker can survive typically for 2 rotations, although with shape, contrast and positions different from previous rotation. In some high resolution images of 2010 elongation a meridional flow was noticed [12], with average drift ~ 5 m/s at $\phi = \pm 10°$. This measurement was quite difficult to do since to minimize the uncertainty the time interval between the images must be great, in order of one or two equatorial rotations, with consequent change of clouds structure due to dynamical processes. The value found is comparable with Venus Express [19] and previous data [12].

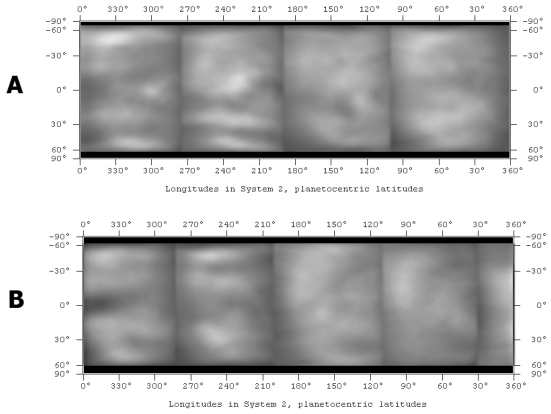

Figure 4: Cylindrical UV maps of April 20-23, 2007 rotation (A) and April 16-19, 2007 rotation (B) considering the average mean period found. The continuity of the clouds during consecutives days is obvious, as well as the dynamical differences between the two rotations, with formation of the Y shaped equatorial cloud at $\lambda \sim 300°$.

4. IR analysis

Clouds visible in near IR light have contrast smaller than those visible in UV [2]. A comparison with UV images taken at same time reveal completely different structures, confirming previous observations [2]. The most frequent feature is a dark, equatorial and latitudinally thin cloud generating close to the subsolar point and sometimes expanding until the terminator (Fig.5). Bright clouds spanning in longitudes and latitudinally thin, often visible in UV images, seem to be rare. The evolution of clouds, even the largest, is faster than UV, with mean life-times generally limited to one-two days. Smallest clouds (< 5" in size) change their shape and brightness in ~ 5 hours. Winds speed were measured on 26-27-28, April 2010 images, choosing 9 latitutes bands with amplitude of $\Delta\phi \sim 4°$, and binning the values. The resulting plot shows a global constant trend in the range $-30° < \phi < +30°$ within the $1-\sigma$ confidence of 14 m/s (Fig.6). Mean wind velocity is found to be $< v >= (73 \pm 5)$ m/s, in agrement with Venus Espress data [16]. The slower value respect to the UV confirm that we are observing clouds at lower altitudes, typically ~ 60 km [2] [12]. Equatorial mean period is then found to be $P = (6,26 \pm 0.45)$d (Fig.7).

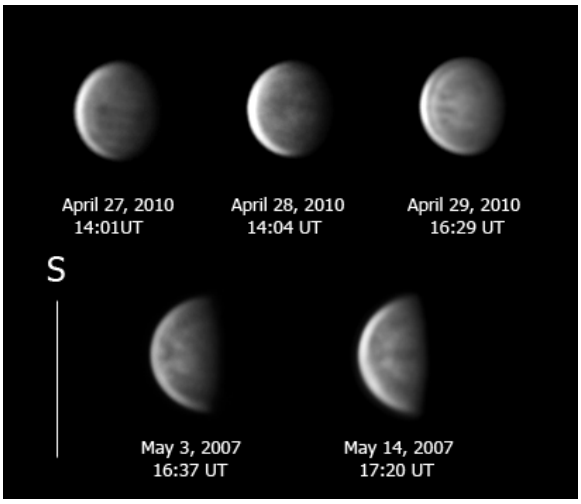

Figure 5: Near IR images showing a common equatorial cloud generating close to the subsolar point, sometimes expanding in longitude and moving with smaller velocity respect to the average trend.

In images of April 29 2010, taken at distance of 4 hours, the dark equatorial cloud descrived earlier was present close to subsolar point longitudes. The measured velocity of these regions gave a value $\sim$ 3.5 times smaller than the mean wind speed found in the ± 15 latitudinal range, and 3 times out the mean standard deviation. The entire zone centered around the cloud has speed smaller than the average. Values outside this region respect the mean trend found earlier (Fig. 6). It is not clear wheter these lower velocities are real or due to dynamical or chemical changes of the cloud, but the absence of this stationary feature the previous and nex day seems to confirm the latter hypotesis. A similar situation was observed in two images taken on May 13-14 2007, when small Y shaped equatorial cloud close to the subsolar point was observed (Fig.5) with similar quasi-static behaviour. Further data are needed to study the dynamics of these clouds. At the countrary of UV images, no direct connections among features are present in images taken on consecutive days, confirming the fast dynamical evolution of clouds. Images taken at time interval of one equatorial mean rotation revealed a quite different global structure. Dark clouds at $\phi \sim \pm 10°$, that generally dominate the images when dark equatorial and longitudinal cloud is not present, seem to undergo to a latitudinal expansion visible in ~ 5 hours. This observation should be investigated by further images.

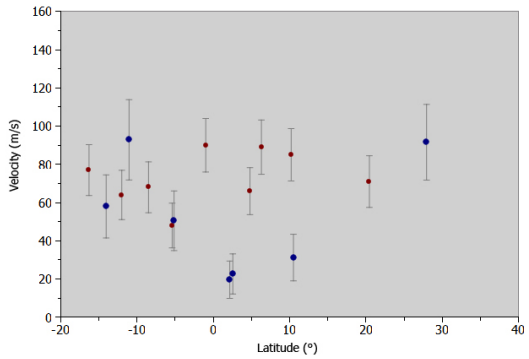

Figure 6: Near infrared winds rotation graph. Red dots are binned values from 3 images. Blue dots are values around small velocity equatorial dark cloud close to the subsolar point, visible in 2010 and 2007.

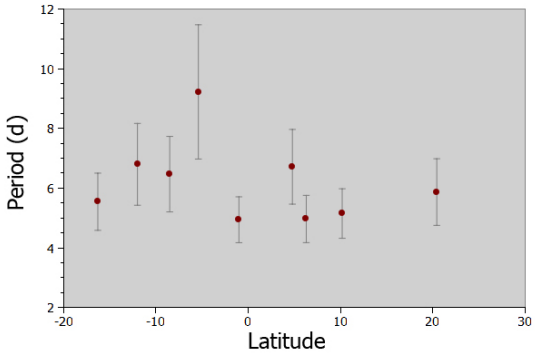

Figure 7: Clouds mean period at 965 nm. Zonal change near the equator are real and sometimes 3 times larger than the average trend.

4.1 The thermal emission

Christophe Pellier was the first amateur to detect the thermal emission of the planet, using a 0.36 m telescope [17]. In the images, Limaye noticed some low contrast large scale spots on the disk, probably correlated with surface features [19]. Unfortunately data did not have enough quality to give further answers. During March 2009 the planet was in perfect geometrycal condition to show the nightside thermal emission, imaged at 1.01 micron transparency window [11] [1] for 7 days in a row, from March 12 to March 18 2009. High quality 16 bit cooled CCD camera was used in order to have a better SNR ratio than Pellier data and to prove the utility of small size telescopes also to these applications. Images calibration and pro-

cessing was performed as descrived earlier. The thermal emission was obvious in any single frame, and every raw image showed some dark features. Details enhancment with unsharp masks and deconvolution was performed. A comparison among the final processed images of the campaign revealed two types of details:

1. small scale (<15"), high contrast, always present, dark spots
2. large scale (generally >15"), low contrast dark features, variable from one day to another.

According to [5][6][11][15][1][17][20], the features visible are mainly due to topography with some zonal contamination by lower cloud layers at altitudes between 30 and 40 km. To prove the surface origin of the smaller, always present, dark spots, the rotation period was estimated. Taking the images of March 12 and 17, and measuring the longitude (λ), with the same technique used for winds estimation, of 10 features, two times each, a solid body rotation was found, with a longitudinal shift of $\Delta\lambda = (6.00 \pm 0.15)^\circ$. Taking into account for the difference due to the elongation between March 12 and 17: $\Delta E = 1.483^\circ$, the rotational period is found to be $P = (240 \pm 6)$ d. This is the confirmation that most of the features belong to the surface, with planetocentric coordinates (system I): $-30^\circ < \phi < 60^\circ$ and $250^\circ < \lambda < 330^\circ$ with C.M. at 329° (average value of the campaign). The limited silicon sensitivity of the CCD did not allow to image the planet at greater wavelengths and erase the clouds contamination, as done by Mueller [16]. Fortunately, clouds lower layers rotates with a rotational period more than one magnitude shorter than the surface [22], then in order to build a better topographic map and show at best surface features, the median of March 16-17-18 processed images was performed. The same procedure was applied to March 12-13-14 images. A cylindrical map of these images and the comparison with Magellan spacecraft altimetric data [9] can be seen in Fig.8. As showed by recent Venus Express data [16] and confirmed here, at 1.01 micron transparency window the contrast difference (i.e. flux variations) of surface spots is regulated mainly by altimetry rather than different mineralogy; coordinates of the main surface features identified are reported in Table 1. Spatial mean resolution was 2.6", while temperature resolution ~ 5 K, a result very similar to that reached by larger ground-based telescopes like the Anglo-Australian observatory [7].

Some photometry was performed on raw calibrated images. Contrast measurement between dark and bright spots was carried by selecting two features near the limb: a dark spot located at $\phi = +29.0^\circ$, $\lambda = 285.0^\circ$, identified as Beta Regio, and a bright spot located between Beta Regio and Phoebe Regio, at $\phi = +11.0^\circ$, $\lambda = 275.0^\circ$. Scattered light correction from the dayside ($\sim 10^4$ times brighter) was performed by tracing the photometric profile along a 90x3 pixel box, just outside the nightside and parallel to dayside cusps, and subtracted to the same box profile centered on the measurement regions. A linear regression was performed to erase the trend; zero point was then found by averaging the values of 80 pixels outside the nightside resulting profile. The measurement of the specific brightness of these regions, on the images taken on March 12-16-17-18, gave a contrast $0.20 < C < 0.30$, in agreement with professional telescopes data [14].

In March 12 session, in the same field of view of the planet, there were two stars: HD3884, $m_v = 7.70 \pm 0.02$, and TYCO610-01641-1 $m_v = 9.36 \pm 0.02$ useful to estimate the instrumental surface magnitude of the nightside with simple aperture photometry. The raw image made of 300 single calibrated exposures was considered and the net intensity of the stars, after subtracting the background with an annulus centered around the stars, was derived. Scattered light correction from the dayside was performed on the nightside as descrived earlier, then mean specific intensity along a 10x3 pixels profile on the nightside was measured. The resulting differential magnitudes were averaged and corrected for the unitary surface 1.35 times greater than the sampling of 0.86 "/px, producing a $\Delta m = -0.32 \pm 0.02$. In order to calculate the instrumental surface magnitude, the instrumental magnitudes of the stars were estimated. Considering the transmission band of the setup between I and J photometric bands, an average V-I and V-J color indices was used. The surface mean magnitude of the nightside is then found to be: $m_i = 10.4 \pm 0.3 mag/arcsec^2$. As stated earlier, it was impossible to discriminate the contribution of the clouds on the single image, but it was possible to show brightness change during time due to difference in opthical depht of fast moving low clouds, as follows. Two raw images shot in consecutives days were considered, with similar SNR, so that the rotation of the surface was negligible at real resolution of 2.6". Correction for differences in orientation and size were performed, then the intensity values were divided, in order to have a new image that showed only photometrical changes (if present). Applying this technique to 16-17-18 March images, the

best of the campaign, all the topography details disappeared, as expected. The resulting images show large scale brightness gradients due to the change in clouds opacity (Fig.9), as noticed also by Venus Express Monitoring Camera [18], and confirming the nature of first type variable features observed in the processed images. The images confirm also the earlier hypothesis that clouds contamination is restricted to some time-dependent areas, focused mainly at equatorial latitudes.

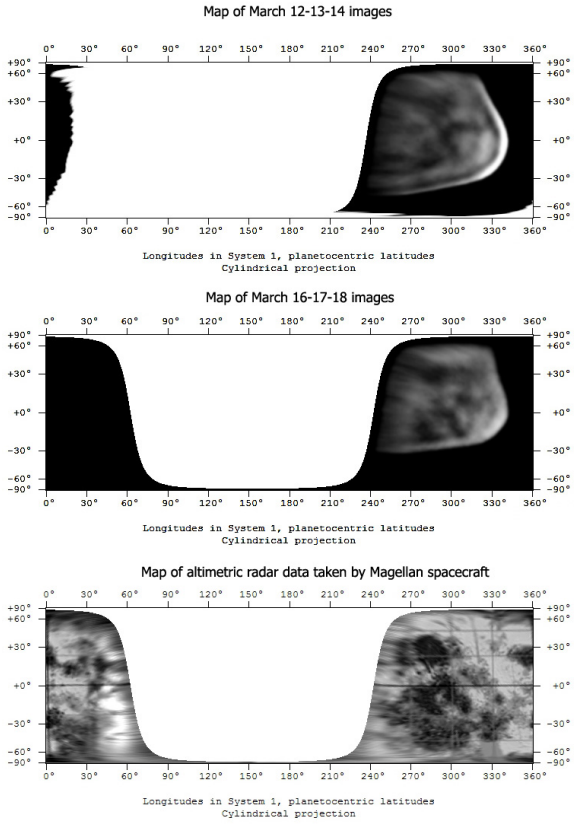

Figure 8: Cylindrical maps of surface features imaged at the transparency window of 1.01 micron and comparison with Magellan altimetric data.

5. Conclusions

It was demonstrated that amateur size telescopes can image the atmosphere and the nightside of the planet with a spatial resolution better than 1" (for the dayside), also during daylight, producing high quality

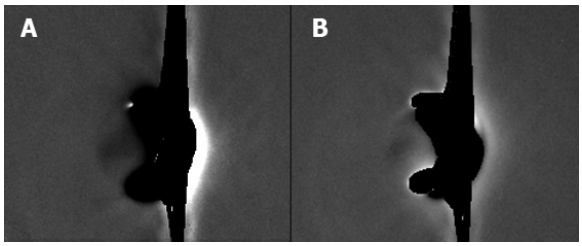

Figure 9: Optical depth change in the nightside. Image A is the division of March 17 and March 16 raw images; image B is the result of the division between March 18 and March 16 images.

Table 1: Planetocentric coordinates of surface features identified in the thermal emission.

Feature	Lat.	Long.
Beta Regio	30	285
Hyndla Regio	30	300
Asteria Regio	20	270
Devana Chasma	15	285
Dolya Tessera	0	300
Phoebe Regio	-5	285
Navka Planitia	-5	310

data of clouds and thermal emission. A continuative campaign will provide more long term data, useful to understand the atmopsherical dynamics and evolution. Increasing the time interval between the observations, uncertainties on the winds speed can be smaller than 10 m/s. Good seeing conditions images set will provide measurements of meridional flow in UV and more data about the zonal velocities in near IR noticed in this paper and in Venus Express and Galileo images [19]. Nightside thermal emission continuative imaging is useful to follow the low layers of the atmosphere and also to monitor the surface looking to change caused by recent or still active lava flows, visible as hot spots in the images [10] or other endogenic processes. Images and data have enough precision to be a solid support to the Venus Express Mission.

References

[1] Baines et al.: Detection of Sub-Micron Radiation from the Surface of Venus by Cassini/VMS, Icarus 148 [2000] 307-11 - thermal emission at 850 and 900 nm from the surface, 2000.

[2] Belton et al. 1991: Images from Galileo of the Venus Cloud Deck, Science 253 [1991 Sep. 27] 1531-6.

[3] Boyer, C. Camichel, Ann. d'Astrophysique, 24, 531, H. 1961.

[4] Boyer, C., Newell, The Astronomical Journal, 72, 679, R. E. 1967.

[5] Carlson, R. W., Baines, K. H., Girard, M., Kamp, L. W., Drossart, P., Encrenaz, T., Taylor, F. W.: Galileo/NIMS near-infrared thermal imagery of the surface of Venus, In Lunar and Planetary Inst., Twenty-fourth Lunar and Planetary Science Conference. Part 1: A-F p 253 (SEE N94-12015 01-91), 1993.

[6] Carlson R. W. et al. 1991: Galileo Infrared Imaging Spectroscopy Measurements at Venus provides a telling NIMS spectrum and quantitative contrast data for the various NIR windows, Science 253 1541-8, 1991 Sep. 27.

[7] Crisp, D., Allen, D. A., Grinspoon, D. H., Pollack, J. B.: Near-infrared images and spectra from the Anglo-Australian Observatory, Science (ISSN 0036-8075), vol. 253, p. 1263-1266, Sept. 13, 1991.

[8] Del Genio, A. D., Rossow, W. B.: Temporal variability of ultraviolet cloud features in the Venus stratosphere, Icarus, Volume 51, Issue 2, Pages 391-415, August 1982.

[9] Ford Peter G. et al.: Venus topography and kilometer-scale slopes, Journal of Geophysical Research (ISSN 0148-0227), vol. 97, no. E8, p. 13,103-13,114, Aug. 25, 1992.

[10] Hashimoto, George L., Imamura, Takeshi: Elucidating the Rate of Volcanism on Venus: Detection of Lava Eruptions Using Near-Infrared Observations, Icarus 154, Issue 2, December 2001, Pages 239-243, 2001.

[11] Lecacheux, J., Drossart, P., Laques, P., Deladerriere, F., Colas, F.: Detection of the surface of Venus at 1.0 μm from ground-based observations, Planet. Space Sci. 41 543-9. 1993.

[12] Limaye, S. S.: Venus atmospheric circulation: Known and unknown, J. Geophys. Res., 112, E04S09, doi:10.1029/2006JE002814, 2007.

[13] McKim, R.: Ground-based support for the Venus Express mission, Journal of the British Astronomical Association, Vol. 116, No. 2, p.60, 2006.

[14] Meadows, V. S. et al.: Groundbased near-IR observations of the surface of Venus, In Lunar and Planetary Inst., Papers Presented to the International Colloquium on Venus p 70-71 (SEE N93-14288 04-91), 1992.

[15] Meadows, V. S., and Crisp D.: Ground-based near-infrared observations of the Venus nightside: The thermal structure and water abundance near the surface, Journal of Geophysical Research 101 E2 4595-4622, 1996.

[16] Mueller, C. L.: Venus Geochemistry: Progress, Prospects, and New Missions, LPI Contribution No. 1470, p.45-46, February 26-27, 2009.

[17] Pellier, C.: Thermal Emission on the Venusian Nightside, www.astrosurf.org/pellier/venusthermal - website with his own observations from May 2004.

[18] Russo, P., Titov, D. V., Markiewicz, W. J., Moissl, R., Ignatiev, N., Keller, H. U., Crisp, D., Basilevsky, A. T.: Imaging of the Venus night side with the Venus Monitoring Camera onboard Venus Express, European Planetary Science Congress 2006, p.428. Berlin, Germany, 18 - 22 September 2006.

[19] Sánchez-Lavega, A., et al.: Variable winds on Venus mapped in three dimensions, Geophys. Res. Lett., 35, L13204, doi:10.1029/2008GL033817, 2008.

[20] Shiga, D.: Amateur Images Venus' Surface, www.skyandtelescope.com/news/article_1266_1.asp, 2004.

[21] Travis, L. D. et al.: Cloud images from the Pioneer Venus Orbiter, Science, vol. 205, July 6, 1979, p. 74-76, 1979.

[22] Young, E. F. et al.: Direct observations of complex cloud motions in Venus' lower atmosphere; GS - AGU - EUG Joint Assembly, Abstracts from the meeting held in Nice, France, 6 - 11 April 2003.